plasma membrane by co-immunoprecipitation assay. CD9 co-precipitated with anti-integrin α6 antibody in lysates from both mouse eggs and F9 cells (Fig. 3D), indicating that CD9 physically associates with integrin α6β1 on egg plasma membrane, as shown in other cell lines (*7*).

The integrin family provides a physical link between the extracellular matrix and the cell cytoskeleton and transduces signals, eliciting changes in the intracellular pH, cytoplasmic calcium level, phospholipid metabolism, protein tyrosine and serine/threonine phosphorylation, and expression of certain genes (*21*). Recent studies suggest that integrin-associated transmembrane proteins, including CD9 and TM4, may also participate in integrin-mediated signaling (*22*). We have shown here that CD9 associates with integrin α6β1 in eggs. Therefore, integrin α6β1 may transduce signals to CD9 and initiate, or otherwise promote, fusion. However, CD9 may directly function in membrane fusion. In support of this possibility, it should be noted that some anti-CD9 or anti-TM4 antibodies block virus-mediated syncytium formations where the involvement of integrin is not clear (*23*).

Our results show that CD9 is a crucial factor for mouse oocytes in fertilization. $CD9^{-/-}$ mice may serve to elucidate the precise mechanism of sperm-egg fusion and the role of CD9-integrin complex.

References and Notes

1. R. Iwamoto, H. Senoh, Y. Okada, T. Uchida, E. Mekada, *J. Biol. Chem.* **266**, 20463 (1991).
2. J. H. Kersey *et al.*, *J. Exp. Med.* **153**, 726 (1981); R. A. Newman, D. R. Sutherland, T. W. Lebien, J. H. Kersey, M. F. Greaves, *Biochim. Biophys. Acta* **701**, 318 (1982); Y. Nakamura, R. Iwamoto, E. Mekada, *Am. J. Pathol.* **149**, 575 (1996); M. Higashiyama *et al.*, *Cancer Res.* **55**, 6040 (1995).
3. H. T. Maecker, S. C. Todd, S. Levy, *FASEB J.* **11**, 428 (1997).
4. A. R. Shaw *et al.*, *J. Biol. Chem.* **270**, 24092 (1995); M. Hadjiargyrou and P. H. Patterson, *J. Neurosci.* **15**, 574 (1995); E. S. Anton, M. Hadjiargyrou, P. H. Patterson, W. D. Matthew, *J. Neurosci.* **15**, 584 (1995); S. Ikeyama, M. Koyama, M. Yamaoko, R. Sasada, M. Miyake, *J. Exp. Med.* **177**, 1231 (1993).
5. K. Nakamura, R. Iwamoto, E. Mekada, *J. Cell Biol.* **129**, 1691 (1995).
6. F. Berditchevski, M. M. Zutter, M. E. Hemler, *Mol. Biol. Cell* **7**, 193 (1996).
7. R. Iwamoto *et al.*, *EMBO J.* **13**, 2322 (1994); S. Higashiyama *et al.*, *J. Cell Biol.* **128**, 929 (1995).
8. A mouse genomic DNA clone containing exons 2 through 8 of the CD9 gene was isolated by screening a genomic DNA library derived from the 129/Sv mouse strain. The targeting vector was prepared using a 10-kb Apa I–Xho I fragment containing exons 3 to 8 of the CD9 gene, PGK-neo-polyA cassette and pBluescript plasmid. This construct was designed to delete a ApaI-BglII fragment from the CD9 gene, encompassing a part of exon 3 to all of exon 4 as schematized in Fig. 1A. The Not I–linearized targeting vector was transfected into the ES line. Five of 300 G418-resistant clones underwent the desired homologous recombination. Two positive clones were injected into blastocysts, and chimeric offspring were mated to C57BL/6J females. Mice carrying the mutation in the heterozygous state ($CD9^{+/-}$) were intercrossed to produce homozygous mutants ($CD9^{-/-}$), and 4- to 8-week-old mice were used for analysis. To determine the genotype of the CD9 locus, DNA samples were extracted from adult tails after digestion with proteinase K and were analyzed by Southern blotting using a labeled probe (Fig. 1B).
9. $CD9^{+/+}$, $CD9^{+/-}$, and $CD9^{-/-}$ females (2 to 3 months old) were caged with one male for 10 days to 2 months, and the number of pups born was counted. Breeding capacities of each genetic background were determined using 4 to 20 pairs of mice of all the genetic combinations.
10. Ovaries dissected from mice were fixed in 4% paraformaldehyde and embedded in paraffin. Sections were stained with hematoxylin and eosin.
11. K. Miyado, K. Inoue, A. Ogura, E. Mekada, data not shown.
12. Mature female mice were superovulated by injecting 5 IU of pregnant mare's serum and 5 IU of hCG at 48-hour intervals. Eggs were collected 13 to 15 hours after the hCG injection from the oviductal ampulla region under paraffin and were placed in a 400 μl drop of TYH medium (*24*) equilibrated with 5% CO_2 in air at 37°C. Zona-free eggs were prepared by acidic tyrode according to the method described [B. Hogan, F. Costantini, E. Lacy, *Manipulating the Mouse Embryo* (Cold Spring Harbor Laboratory, Cold Spring Harbor, NY, 1986)]. In some of the experiments, eggs were incubated with antibodies for 30 min before sperm insemination. Antibodies were present throughout sperm-egg incubations. Sperm collected from the cauda epididymidis of mature male mice were suspended in 400 μl of TYH medium and preincubated for 90 min before adding to eggs. The final concentrations of sperm added to the eggs were 1×10^5 to 1.5×10^5 sperm/ml.
13. R. Yanagimachi, in *The Physiology of Reproduction*, E. Knobil and J. D. Neil, Eds. (Raven Press, New York, 1994), pp. 189–317; P. M. Wassarman, *Science* **235**, 553 (1987).
14. In order to observe the fusion, the eggs were fixed with 0.05% glutalaldehyde and 10% formaldehyde followed by staining with 0.5% lacmoid (*24*).
15. Fusing ability of $CD9^{-/-}$ and $CD9^{+/+}$ eggs with wild-type sperm was also determined by dye transfer assay (*17*). By this assay, fusion with sperm was not observed in $CD9^{-/-}$ eggs ($n = 9$), whereas 100% of $CD9^{+/+}$ eggs ($n = 10$) fused with sperm (average of 1.6 sperm per egg).
16. Mature eggs collected from $CD9^{+/+}$ or $CD9^{-/-}$ females, as described above (*12*), were freed from cumulus cells by treatment with bovine testicular hyaluronidase in CZB medium [C. L. Chatot *et al.*, *J. Reprod. Fertil.* **86**, 679 (1989)]. The eggs were each injected with the head of epididymal spermatozoa from mature C57BL/6J males by using Piezo micromanipulator as reported [T. Wakayama *et al.*, *Nature Biotechnol.* **16**, 639 (1998)]. After 24 hours of culture in CZB medium under 5% CO_2 in air at 37°C, eggs that developed to the two-cell stage were transferred into the oviducts of day-1 pseudopregnant ICR females. The recipient females were allowed to deliver young.
17. E. A. Almeida *et al.*, *Cell* **81**, 1095 (1995).
18. W. J. Snell and J. M. White, *Cell* **85**, 629 (1996); D. Bigler, M. Chen, S. Waters, J. M. White, *Trends. Cell Biol.* **7**, 220 (1997); J. P. Evans *et al.*, *Biol. Reprod.* **59**, 145 (1998); D. G. Myles and P. Primakoff, *Biol. Reprod.* **56**, 320 (1997).
19. C. Cho *et al.*, *Science* **140**, 1857 (1998).
20. H. Chen and N. S. Sampson, *Chem. Biol.* **6**, 1 (1998).
21. A. Howe, A. E. Aplin, S. K. Alahari, R. L. Juliano, *Curr. Opin. Cell Biol.* **10**, 220 (1998).
22. M. E. Hemler, *Curr. Opin. Cell Biol.* **10**, 578 (1998).
23. K. Fukudome *et al.*, *J. Virol.* **66**, 1394 (1992); S. Loffler *et al.*, *J. Virol.* **71**, 42 (1997).
24. Y. Toyoda, M. Yokoyama, T. Hoshi, *Jpn. J. Anim. Reprod.* **16**, 147 (1971).
25. Anti-diphtheria toxin antibody no. 2 [S. Hayakawa, T. Uchida, E. Mekada, M. R. Moynihan, Y. Okada, *J. Biol. Chem.* **258**, 4311 (1983)].

26. We thank S. Kaur and members of Chrysalis DNX Transgenic Science Inc. for producing knockout mice, K. Miyake for providing anti-CD9 antibody KMC8.8, M. Kimoto for suggestions, and the members of the department of Immunology, Saga Medical School, for suggestions and analysis of bone marrow cells. Supported in part by a grant from The Research for the Future Program, the Japan Society for the Promotion of Science (JSPS) (project 97L00303), and a Grant-in Aid for Scientific Research, The Ministry of Education, Science, Sports and Culture (grant 09480198) for E.M. All animal care and experiments were in accordance with Kurume University and Osaka University Animal Care and Use Committee guidelines.

6 October 1999; accepted 29 November 1999

Regulation of JNK by Src During *Drosophila* Development

Minoru Tateno, Yasuyoshi Nishida, Takashi Adachi-Yamada*

In *Drosophila*, the Jun amino-terminal kinase (JNK) homolog Basket (Bsk) is required for epidermal closure. Mutants for *Src42A*, a *Drosophila* c-*src* protooncogene homolog, are described. Src42A functions in epidermal closure during both embryogenesis and metamorphosis. The severity of the epidermal closure defect in the *Src42A* mutant depended on the amount of Bsk activity, and the amount of Bsk activity depended on the amount of Src42A. Thus, activation of the Bsk pathway is required downstream of Src42A in epidermal closure. This work confirms mammalian studies that demonstrated a physiological link between Src and JNK.

Genes that regulate cell shape changes in *Drosophila* are required for dorsal closure of the embryonic epidermis and thorax closure of the pupal epidermis (*1*). Mutations in genes such as *hemipterous* (*hep*) and *basket* (*bsk*, also known as *DJNK*) result in abnormal embryos with a dorsal hole or abnormal adults with a dorsal midline cleft (*1*, *2*). Hep and Bsk are homologous to the mammalian MKK7 (MAPK kinase 7) and JNK, and they are components of a MAPK (mitogen-activated protein kinase) cascade (*3*). Although the role of the Hep-Bsk cascade during dorsal closure has been extensively studied, the up-

Division of Biological Science, Graduate School of Science, Nagoya University, Chikusa-ku, Nagoya 464-8602, Japan.

*To whom correspondence should be addressed. E-mail: adachi@bio.nagoya-u.ac.jp

stream trigger of this cascade is poorly understood. To identify the trigger, we screened mutants showing the dorsal midline cleft phenotype, like a mild *hep* mutant (Fig. 1Ab). We found that the mutant for *Src42A* showed this phenotype and that Src42A regulates Bsk during *Drosophila* development.

From our mutant collection of the P-element–inserted semilethal lines, we identified one line, *Jp45*, that survived to adulthood but showed various degrees of the dorsal midline cleft phenotype (Fig. 1A, c to e). Excision of the P-element eliminated the semilethality and restored the cleft phenotype. The P-element was inserted in the 5′ untranslated region (UTR) of the *Src42A* gene, which encodes a Src-family nonreceptor tyrosine kinase (*4*–*6*). We used ethyl methanesulfonate (EMS) mutant screening to isolate two strong alleles of *Src42A*, $Src42A^{E1}$ and $Src42A^{myristylation\ (myri)}$ (*7*). In $Src42A^{E1}$, a stop codon at codon 483 eliminated the COOH-terminal part of the kinase domain of Src42A (*8, 9*). $Src42A^{myri}$ has a point mutation in codon 2, which causes an amino acid substitution from Gly^2 to Asp. Gly^2 is conserved in all members of the Src family and must be myristylated for localization of Src to the cellular membrane in mammals (*10*). About 50% of the $Src42A^{myri}$ homozygotes died before they hatched (Table 1), and most of the remainder died during the first-instar larval stage. Therefore, Gly^2 is required for development.

Because adult $Src42A^{Jp45}$ phenotypes resembled that of *hep*, we suspected that Src42A was involved in Hep and Bsk function. A mutation in *hep* or *bsk* dominantly enhanced the lethality and the phenotypic severity of $Src42A^{Jp45}$ homozygotes (Table 2 and Fig. 1B). Conversely, reducing the gene dosage of *puckered* (*puc*), a gene encoding a phosphatase that inactivates Bsk (*11*), suppressed the lethality and the severity of the cleft phenotype of $Src42A^{Jp45}$. Thus, Src42A may function in the Bsk pathway during metamorphosis.

Dorsal closure is the process in which a pair of epidermal layers elongates dorsally and fuses at the dorsal midline of the embryo (*1*) (Fig. 1Ca). This process is not completed in *hep* and *bsk* mutants, yielding a dorsal open phenotype (Fig. 1Cb). Strong *Src42A* mutants did not show the dorsal open phenotype but displayed the malformed mouth parts (Fig. 1Cc). This defect is similar to the defect in the embryo of the *Tec29* mutant (Fig. 1Cd) (*12*). Tec29 is a Src-related nonreceptor tyrosine kinase and is regulated by SRC64, another *Drosophila* Src

Table 1. Synergism of *Src42A* and *Tec29* found in embryonic lethality.

Genotype	Embryonic lethality* (±SE) (%)	N†
$Src42A^{E1}/Src42A^{E1}$	75.7 (±3.6)	576
$Src42A^{myri}/Src42A^{myri}$	50.0 (±3.3)	908
$Tec29^{206}Tec29^{5610}$	28.2 (±3.0)	895
$Tec29^{206}\ Src42A^{myri}/Tec29^{5610}\ Src42A^{myri}$	105.8 (±1.1)	1925
Wild type	0.2 (±0.2)	937

*Percentage of embryonic lethality = (number of unhatched embryos × 400)/(total number of embryos). †Total number of embryos is shown.

Table 2. Effect of *Tec29*, *hep*, *bsk*, and *puc* mutations on *Src42A* mutant lethality. All crosses were performed at 18°C because the viability of $Src42A^{Jp45}$ was reduced at 25°C, the standard temperature.

Genotype	Viability (±SE) (%)	N*
$Src42A^{Jp45}/Src42A^{Jp45}$	2.8 (±0.3)	3465.5
$hep^{r75}/+;\ Src42A^{Jp45}/Src42A^{Jp45}$	1.1 (±0.3)	1126.5
$bsk^2\ Src42A^{Jp45}/+\ Src42A^{Jp45}$	0.1 (±0.1)	1978
$Src42A^{Jp45}/Src42A^{Jp45};\ puc^{E69}/+$	36.1 (±2.2)	484.5
$Tec29^{206}\ Src42A^{Jp45}/+\ Src42A^{Jp45}$	0.0	1033
$Tec29^{5610}\ Src42A^{Jp45}/+\ Src42A^{Jp45}$	0.0	1589.5

*The theoretically expected number (*N*) of each mutant as a result of the crossing was determined from the number of phenotypically normal siblings.

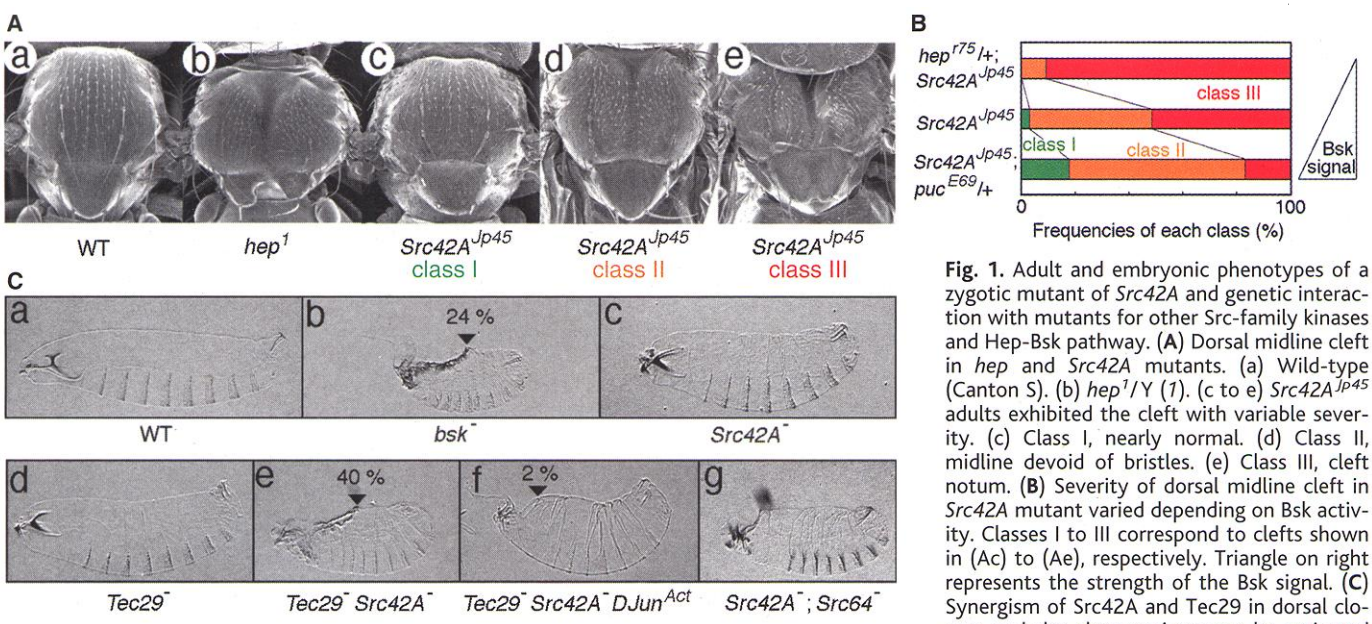

Fig. 1. Adult and embryonic phenotypes of a zygotic mutant of *Src42A* and genetic interaction with mutants for other Src-family kinases and Hep-Bsk pathway. (**A**) Dorsal midline cleft in *hep* and *Src42A* mutants. (a) Wild-type (Canton S). (b) hep^1/Y (*1*). (c to e) $Src42A^{Jp45}$ adults exhibited the cleft with variable severity. (c) Class I, nearly normal. (d) Class II, midline devoid of bristles. (e) Class III, cleft notum. (**B**) Severity of dorsal midline cleft in *Src42A* mutant varied depending on Bsk activity. Classes I to III correspond to clefts shown in (Ac) to (Ae), respectively. Triangle on right represents the strength of the Bsk signal. (**C**) Synergism of Src42A and Tec29 in dorsal closure and the phenotypic rescue by activated DJun. (a) Wild-type. (b) bsk^2. Arrowheads in (b), (e), and (f) mark the posterior edge of the dorsal hole in the cuticles. Percentage of embyros in which the posterior edge of the dorsal hole extended posterior to the 50% length of the embryo is indicated. (c) A $Src42A^{myri}$ homozygote. A similar mouth part defect was observed in $Src42A^{E1}$. (d) $Tec29^{206}/Tec29^{5610}$ trans-heterozygote. (e) $Tec29^{206}\ Src42A^{myri}/Tec29^{5610}\ Src42A^{myri}$. (f) $Tec29^{206}\ Src42A^{myri}\ sevE(hs)\text{-}DJun^{Act}/Tec29^{5610}\ Src42A^{myri}$. A larger proportion of the embryos of this genotype had a small anterior hole, as shown. (g) $Src42A^{myri};\ Src64^{P1}$.

homolog, during oogenesis (*13*). Thus, Tec29 may be involved in the function of Src42A. A mutation in *Tec29* dominantly enhanced the lethality of *Src42A*^{Jp45} (Table 2).

Furthermore, the *Tec29 Src42A* double mutant showed complete embryonic lethality (Table 2), and a certain part of the dead embryos showed the dorsal open phenotype (Fig. 1Ce) (*2*). Activated DJun, a transcription factor downstream of Bsk (*14*, *15*), partially rescued the dorsal open phenotype in the *Tec29 Src42A* double mutant (Fig. 1Cf). Thus, Src42A appears to regulate Bsk in the fusion of epithelial sheets during embryogenesis and metamorphosis, and Tec29 is involved in this regulation. We further observed the double mutant for *Src64* and *Src42A*. It manifested a mild but clear dorsal open phenotype (Fig. 1Cg), which suggests a functional redundancy between Src64 and Src42A.

Expression of *puc* is known to be induced by the Bsk signal (*2*, *11*). In the wing disc of the wild-type third-instar larva, *puc* is expressed in the dorsal midline of the adult notum (Fig. 2Aa) (*16*). In the wing disc of the *Src42A*^{Jp45} mutant, *puc* expression was reduced (Fig. 2Ab). In contrast, larvae with a constitutively activated form of Src42A (Src42A^{CA}) (*17*) showed ectopic expression of *puc* (*18*, *19*) (Fig. 2Ac). Further, introduction of a *hep* null mutation reduced the amount of ectopic *puc* expression (Fig. 2Ad). It is known that Bsk induces expression of *puc* and *decapentaplegic* (*dpp*) during embryonic dorsal closure (Fig. 2B, a and c) (*2*, *11*, *14*, *15*). The embryos of the *Tec29 Src42A* double mutant did not show any *puc* or *dpp* expression in the leading edge cells (Fig. 2B, b and d) (*20*). These results indicate that Src42A, Tec29, Hep, and Bsk regulate *dpp* and *puc* expression during embryonic dorsal closure.

To investigate the ability of Src42A^{CA} to activate Bsk, we directly assessed the amount of phosphorylated Bsk by immunoblot analysis (*21*). Forced expression of Src42A^{CA} did not affect the quantity of total Bsk protein (Fig. 2C, upper lanes) but induced more phosphorylated Bsk (Fig. 2C, lane 4) than the controls. Thus, Src42A appears to regulate the phosphorylation level of Bsk.

During embryonic dorsal closure, the Hep-Bsk signal is required for elongation of the leading edge cells (*1*). In the absence of the Bsk signal, these cells do not fully elongate (*2*). The accumulation of F-actin and phosphotyrosine (P-Tyr) in leading edge cells is associated with the elongation of these cells (Fig. 2D, a and c). Accumulation of these substances is disturbed in the *DJun* and the *puc* mutants (*11*, *15*). In the double mutant for *Tec29* and *Src42A*, the leading edge cells contained reduced quantities of F-actin and P-Tyr, and these cells were only partially elongated (Fig. 2D, b and d). Thus, the defect in embryonic dorsal closure in the *Tec29 Src42A* double mutant is caused by this failure in cell shape change, as is the case in the *DJun* mutant.

We propose a model in which Src42A, upon receiving an unidentified signal, activates the Hep-Bsk pathway to regulate cell shape change and epidermal layer movement. This is consistent with the observation in mammals that c-Src regulates the cell morphogenetic and migratory processes and is known to activate JNK (*22*). As in *Drosophila*, c-Src definitely affects F-actin organization and P-Tyr localization during cell morphogenesis (*23*). Therefore, Src regulation of JNK activity toward a change in cell shape may be conserved.

It can be also interpreted that Src42A acts upstream of DFos (*24*), a dimerization partner of DJun. Although the *Src42A*, *Tec29*, and *Src64* single mutants do not show a dorsal open phenotype (*12*, *25*, *26*), the *DFos* mutant clearly exhibits it. This relationship is also analogous to that in mammals. Both c-*src* and c-*fos* knockout mice had a similar defect, osteopetrosis caused by reduced osteoclast function. But the phenotypic severity was milder in c-*src* than in c-*fos* knockouts (*27*), which can be explained by the functional overlap in multiple Src-family tyrosine kinases (*28*). Accordingly, in both *Drosophila* and mammals, multiple nonreceptor tyrosine kinases may cooperate to regulate the function of the Jun/Fos complex.

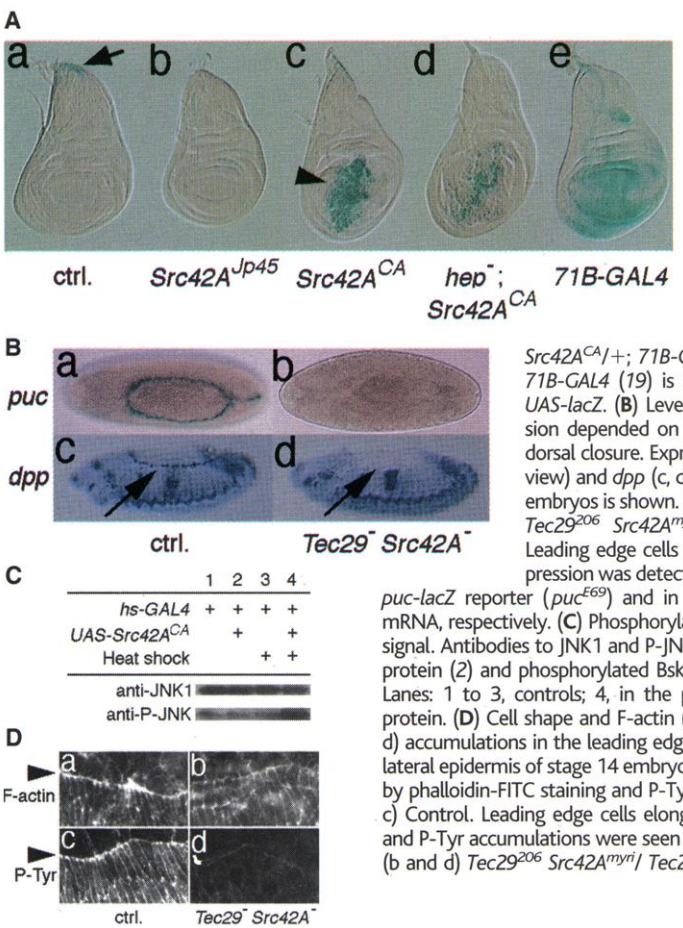

Fig. 2. Regulation of the Bsk pathway and cell shape change by Src42A. (**A**) *puc* expression in wing discs depended on the strength of the Src42A signal. (a) Control. Normal *puc* expression (arrow). (b) *Src42A*^{Jp45}. (c) *UAS-Src42A*^{CA}*/+; 71B-GAL4/+*. Ectopic *puc* expression (arrowhead) (*20*). (d) *hep*^{r75}*/Y; UAS-Src42A*^{CA}*/+; 71B-GAL4/+*. (e) Region where *71B-GAL4* (*19*) is expressed is visualized by *UAS-lacZ*. (**B**) Levels of *puc* and *dpp* expression depended on Src42A and Tec29 during dorsal closure. Expression of *puc* (a, b) (dorsal view) and *dpp* (c, d) (lateral view) in stage 14 embryos is shown. (a and c) Control. (b and d) *Tec29*^{206} *Src42A*^{myri}*/ Tec29*^{5610} *Src42A*^{myri}. Leading edge cells (arrows). *puc* and *dpp* expression was detected by X-gal staining of the *puc-lacZ* reporter (*puc*^{E69}) and in situ hybridization to *dpp* mRNA, respectively. (**C**) Phosphorylation of Bsk by the Src42A signal. Antibodies to JNK1 and P-JNK crossreact with total Bsk protein (*2*) and phosphorylated Bsk protein (*21*), respectively. Lanes: 1 to 3, controls; 4, in the presence of the Src42A^{CA} protein. (**D**) Cell shape and F-actin (a and b) and P-Tyr (c and d) accumulations in the leading edge cells (arrowheads) of the lateral epidermis of stage 14 embryos. Cell shape was observed by phalloidin-FITC staining and P-Tyr antibody staining. (a and c) Control. Leading edge cells elongated dorsally, and F-actin and P-Tyr accumulations were seen in the cellular membranes. (b and d) *Tec29*^{206} *Src42A*^{myri}*/ Tec29*^{5610} *Src42A*^{myri}.

References and Notes

1. S. Noselli, *Trends Genet.* **14**, 33 (1998); J. Zeitlinger and D. Bohmann, *Development* **126**, 3947 (1999). In the wild-type fly, the pair of wing discs fuses along the dorsal midline to make a continuous cell sheet during metamorphosis (Fig. 1A). Failure of this event leads to the cleft defect.
2. B. Glise, H. Bourbon, S. Noselli, *Cell* **83**, 451 (1995); H. K. Sluss *et al.*, *Genes Dev.* **10**, 2745 (1996); J. R. Riesgo-Escovar, M. Jenni, A. Fritz, E. Hafen, *Genes Dev.* **10**, 2759 (1996).
3. Y. T. Ip and R. J. Davis, *Curr. Opin. Cell Biol.* **10**, 205 (1998).
4. Sequencing analysis revealed that P-*lac*W, a derivative of P-element, was inserted at about base 40 of the 5′-UTR of the *Src42A* (*Dsrc41*) gene.
5. F. Takahashi, S. Endo, T. Kojima, K. Saigo, *Genes Dev.* **10**, 1645 (1996).
6. X. Lu and Y. Li, *Dev. Biol.* **208**, 233 (1999). The *Src42A* gene was previously referred to as *Dsrc41* because of mismapping of region 41 (*5*). In situ chromosomal hybridization revealed that the gene was located in the 42A polytene region (*29*). A genetic complementation test with a series of chromosome 2 deficiencies assigned the *Src42A*^{Jp45} mutation to the 42A1-A3 region (*29*). Also, the *Dsrc41*$^{+}$ transgene (*sE-Dsrc41*+WT-A) partially rescued the phenotype of the strong and mild *Src42A* mutants, which indicates that *Src42A* and *Dsrc41* are the same gene. The recently reported *Src42A* alleles *l (2)10108* and *SK2-4* (*S-382* and *S-527*) failed to complement our *Src42A* alleles. The DNA segment flanking the P-element was obtained by the plasmid rescue method.
7. We used the *Src42A*^{r43} allele for EMS mutant screen-

ing. *Src42A*^{r43} is viable and is the mildest allele among the imprecisely excised lines derived from *Src42A*^{lp45}. Genomic Southern blot analysis revealed no detectable rearrangement around the P-element–inserted region in *Src42A*^{r43}. Because about 10% of the hemizygotes for *Src42A*^{r43} (*Src42A*^{r43}/*Deficiency*) survived to become fertile adult flies with a mild dorsal midline cleft, we screened about 30,000 *Src42A*^{r43} heterozygous flies carrying an EMS-mutagenized chromosome to identify the strong *Src42A* mutant alleles based on the appearance of the mild dorsal midline cleft.

8. S. R. Hubbard, L. Wei, L. Ellis, W. A. Hendrickson, *Nature* **372**, 746 (1994).
9. We extracted total RNA from heterozygous mutant flies, and amplified the *Src42A* coding sequence by reverse transcription polymerase chain reaction (PCR). Then we cloned the products according to standard procedures. For each mutant, we sequenced five independent clones. Mutations found in at least two clones were not considered to be a PCR artifact; we considered them to be the mutations that occurred as a result of EMS mutagenesis.
10. M. D. Resh, *Cell* **76**, 411 (1994).
11. E. Martín-Blanco *et al.*, *Genes Dev.* **12**, 557 (1998).
12. E. M. Roulier, S. Panzer, S. K. Beckendorf, *Mol. Cell* **1**, 819 (1998).
13. M. A. Simon, B. Drees, T. Kornberg, J. M. Bishop, *Cell* **42**, 831 (1985); D. J. Guarnieri, G. S. Dodson, M. A. Simon, *Mol. Cell* **1**, 831 (1998).
14. J. R. Riesgo-Escovar and E. Hafen, *Genes Dev.* **11**, 1717 (1997).
15. X. S. Hou, E. S. Goldstein, N. Perrimon, *Genes Dev.* **11**, 1728 (1997).
16. S. Campuzano and J. Modolell, *Trends Genet.* **8**, 202 (1992).
17. T. E. Kmiecik and D. Shalloway, *Cell* **49**, 65 (1987); H. Piwnica-Worms, K. B. Saunders, T. M. Roberts, A. E. Smith, S. H. Cheng *Cell* **49**, 75 (1987); C. A. Cartwright, W. Eckhart, S. Simon, P. L. Kaplan, *Cell* **49**,83 (1987). The DNA sequence encoding the constitutively active form of Src42A (Src42A^{CA}), which has an amino acid substitution of Tyr^{511} to Phe, was generated by in vitro mutagenesis and cloned into pUAST, the GAL4-responsive vector (*18*). Tyr^{511} corresponds to the negative-regulatory COOH-terminal Tyr of c-Src, and this substitution is known to cause constitutive activation of c-Src.
18. A. H. Brand and N. Perrimon, *Development* **118**, 401 (1993).
19. *UAS-Src42A*$^{CA\ III\text{-}3}$ was driven by *71B-GAL4* driver, which was expressed in the primordial wing pouch [(*18*), Fig. 2Ae]. *puc-lacZ* expression was detected by 5-bromo-4-chloro-3-indolyl β-D-galactopyranoside (X-gal) staining.
20. In all experiments to observe embryos, we used blue balancers (*CyO*, *wg-lacZ* and *TM3*, *Ubx-lacZ*) to identify the genotypes of the embryos. We stained the embryos with X-gal and then with phalloidin-fluorescein isothiocyanate (FITC), or we double-stained them with β-Gal and P-Tyr antibodies, or we double-stained them with the antisense probes of β-galactosidase and *dpp*.
21. *UAS-Src42A*$^{CA\ III\text{-}6}$ was driven by *hs-GAL4*, a heat shock-inducible GAL4 driver (*18*). Larvae were heat-shocked at 37°C for 30 min in a water bath and allowed to recover at 25°C for 2 hours before processing. The larvae were homogenized in a solution of 20 mM tris-HCl (pH 7.4), 1% Triton X-100, 60 mM β-glycerophosphate, 10 mM EGTA, 10 mM $MgCl_2$, 15 mM NaF, 1 mM dithiothreitol, 1 mM Na_3VO_4, 1 mM phenylmethylsulfonyl fluoride, aprotinin (20 μg/ml), pepstatin (1 μg/ml), and leupeptin (1 μg/ml), and then ultracentrifuged (80,000*g*, 45 min, 4°C). We purchased JNK1 and P-JNK antibodies from Santa Cruz Biotechnology (Santa Cruz, CA) and Promega (Madison, WI), respectively. We used a 1:300 dilution of both antibodies. We confirmed that the intensity of the band detected by the P-JNK antibody was elevated after ultraviolet irradiation to larvae, as previously reported by J. R. Riesga-Escovar *et al.* (*2*).
22. M. Nagao, J. Yamauchi, Y. Kaziro, H. Itoh, *J. Biol. Chem.* **273**, 22892 (1998); C. R. Hauck, T. Meyer, F. Lang, E. Gulbins, *EMBO J.* **17**, 443 (1998); I. Timokhina, H. Kissel, G. Stella, P. Besmer, *EMBO J.* **17**, 6250 (1998); S. M. Thomas and J. S. Brugge, *Annu. Rev. Cell Dev. Biol.* **13**, 513 (1997); J. Y.-J. Shyy and S. Chien , *Curr. Opin. Cell Biol.* **9**, 707 (1997); J. M. Rodier, A. M. Vallés, M. Denoyelle, J. P. Thiery, B. Boyer, *J. Cell Biol.* **131**, 761 (1995).
23. S. M. Thomas, P. Soriano, A. Imamoto, *Nature* **376**, 267 (1995); K. B. Kaplan, J. R. Swedlow, D. O. Morgan, H. E. Varmus, *Genes Dev.* **9**, 1505 (1995).
24. J. R. Riesgo-Escovar and E. Hafen, *Science* **278**, 669 (1997).
25. Germ line clones of the *Src42A*^{myri} allele were obtained by x-ray irradiation. When the embryos were zygotically heterozygous for *Src42A*^{myri}, they developed to normal adult flies. On the other hand, 50% of the embryos zygotically homozygous for *Src42A*^{myri} failed to hatch. The dead embryos showed a defect in mouth parts indistinguishable from the regular zygotic mutant. The remaining hatched animals died during the larval stage, which is similar to the case in the regular zygotic mutant. A similar result has been reported by Lu and Li (*6*). In addition, these results are consistent with the suggestion of Takahashi *et al.* (*5*); mRNA of *Src42A* could not be detected at a very early embryonic stage, which indicates the absence of maternal mRNA.
26. G. S. Dodson, D. J. Guarnieri, M. A. Simon, *Development* **125**, 2883 (1998).
27. P. Soriano, C. Montgomery, R. Geske, A. Bradley, *Cell* **64**, 693 (1991); R. S. Johnson, B. M. Spiegelman, V. Papaioannou, *Cell* **71**, 577 (1992); Z. Q. *Wang et al.*, *Nature* **360**, 741 (1992).
28. P. L. Stein, H. Vogel, P. Soriano, *Genes Dev.* **8**, 1999 (1994).
29. M. Tateno, unpublished data.
30. Supported by grants from the Japan Society of Promotion of Science; the Ministry of Education, Science, Sports and Culture of Japan; the Japan Science and Technology Corporation, the Mitsubishi Foundation; and the Kurata Foundation. We thank N. Perrimon, S. Noselli, D. Yamamoto, Y. H. Inoue, M. Therrien, T. Laverty, G. M. Rubin, M. Ooyama, K. Saigo, S. Dodson, M. A. Simon, M. Mlodzik, and the Bloomington Stock Center for the fly strains; N. Perrimon, T. Uemura, Y. Tomoyasu, and M. Nakamura for the plasmid DNAs; N. H. Brown for cDNA library; I. Sugimura and Y. Madoka for technical advice; K. Matsumoto and S. Urushiyama for helpful comments on the manuscripts; and members of our lab for assisting in this work.

14 September 1999; accepted 18 November 1999